

LA-UR-77-1758

*CONFIDENTIAL - 13*  
**TITLE: DECAY HEAT MEASUREMENTS BY FAST-RESPONSE BOIL-OFF**

**CALORIMETRY**

**AUTHOR(S): J. L. Yarnell and P. J. Pendl**

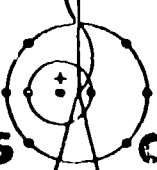
**SUBMITTED TO: ANS Thermal Reactor Safety Meeting**

**Sun Valley, ID, July 31 - August 5, 1977**

**NOTICE**  
This report was prepared as an account of work sponsored by the United States Government. Neither the United States nor the United States Energy Research and Development Administration nor any of their employees, nor any of their contractors, subcontractors, or their employees makes any warranty, express or implied, or assumes any legal liability or responsibility for the accuracy, completeness, or usefulness of any information, apparatus, product, process, disclosure, or representation that may be contained in this document. Reference herein to any privately owned rights

By acceptance of this article for publication, the publisher recognizes the Government's (license) rights in any copyright and the Government and its authorized representatives have unrestricted right to reproduce in whole or in part said article under any copyright secured by the publisher.

The Los Alamos Scientific Laboratory requests that the publisher identify this article as work performed under the auspices of the USERDA.



**los alamos**  
scientific laboratory  
of the University of California  
LOS ALAMOS, NEW MEXICO 87544

An Affirmative Action/Equal Opportunity Employer

ER

Form No. 836  
St. No. 2629  
1/75

UNITED STATES  
ENERGY RESEARCH AND  
DEVELOPMENT ADMINISTRATION  
CONTRACT W-7405-ENG-36

DECAY HEAT MEASUREMENTS

BY FAST-RESPONSE BOIL-OFF CALORIMETRY

BY

J. L. Yarnell and P. J. Bendt

Los Alamos Scientific Laboratory, University of California

Los Alamos, NM 87545

ABSTRACT

A liquid-helium boil-off calorimeter with a 1-s time constant was used to measure  $^{235}\text{U}$  fission product decay heat at times between 10 and  $10^5$  s following a  $2 \times 10^4$  s thermal neutron irradiation. The uncertainty in the data was  $\sim 2\%$  ( $1\sigma$ ) except at the shortest cooling times, where it rose to  $\sim 4\%$ .

We report calorimetric measurements of fission product decay heat, with emphasis on short cooling time. This work is part of a program sponsored by the U. S. Nuclear Regulatory Commission to provide better values and reduced uncertainties for the decay heat source term, for use in reactor safety evaluations, and, in particular, for the analysis of the Loss-of-Coolant Accident (LOCA).

Calorimetric measurements have the advantage that they are relatively simple and straightforward, and thus present a minimum opportunity for the introduction of systematic errors. Their disadvantages are that they provide only integral information (total decay heat, not  $\beta$  and  $\gamma$  spectra), and that, in general, they tend to have long time constants.

Our measurements were carried out with a cryogenic boil-off calorimeter. In this technique, decay heat is used to evaporate a cryogen, in our case liquid helium, and the rate at which boil-off gas is evolved is measured with a fast-response flowmeter. Since the heat of vaporization of helium is known, the amount of decay heat may be calculated from the boil-off rate. Direct calibration by means of electrical heating provides a check on these calculations.

Although the idea of boil-off calorimetry is an old one, we chose it because it offered an opportunity to develop a calorimeter with a short thermal time constant. By operating nearly isothermally, and by taking advantage of the large reduction in the heat capacity of solids which occurs at the temperature of liquid helium (4 K), we were able to achieve a time constant of less than one second in a calorimeter which contained a 52-kg radiation absorber.

Samples of  $^{235}\text{U}$  and  $^{239}\text{Pu}$ , each weighing  $\sim 60$  mg and encased in cladding to retain gaseous fission products, were irradiated for  $2 \times 10^4$  s in a constant thermal-neutron flux of  $3 \times 10^{13}$  n/cm $^2$  s. They were then transferred to the calorimeter in  $\sim 1$  s, and had reached the temperature of liquid helium after an additional 3 s. Decay heat data were obtained for cooling times between  $10$  and  $10^5$  s. After the calorimetric measurements were completed, the number of fissions in the samples was determined radiochemically.

Corrections to the data were made for the leakage of gamma radiation from the calorimeter (3% maximum) and for the initial transient (3.4% maximum). The overall uncertainty ( $1\sigma$ ) in the experimental data is estimated to be  $\sim 2\%$  except at the shortest cooling times, where it rises to  $\sim 4\%$ . The measurements on  $^{235}\text{U}$  have been completed, and those on  $^{239}\text{Pu}$  are in progress.

The experimental data for a  $2 \times 10^4$  s thermal neutron irradiation of  $^{235}\text{U}$  agree within the errors with summation calculations based on the ENDF/B-IV data base. The experimental data were extended to the case of an infinite irradiation by adding the calculated decay heat due to those fissions which took place before the experimental irradiation interval of  $2 \times 10^4$  s. The extended data for infinite irradiation are in good agreement with the summation calculation.

Both the extended experimental data and the summation calculations are significantly ( $\sim 7\%$ ) below the current ANS Decay Heat Standard at short cooling times. This standard, plus 20%, is currently used in reactor safety evaluations.

A preliminary report of our decay heat measurements was presented at the Fourth Water Reactor Safety Information Meeting in September, 1976. A complete description of these measurements is given in The Los Alamos Scientific Laboratory Report LA-NUREG-6713, July 1977 (in publication).

The details of the experiment and its results are indicated in the following Figures and in the Table.

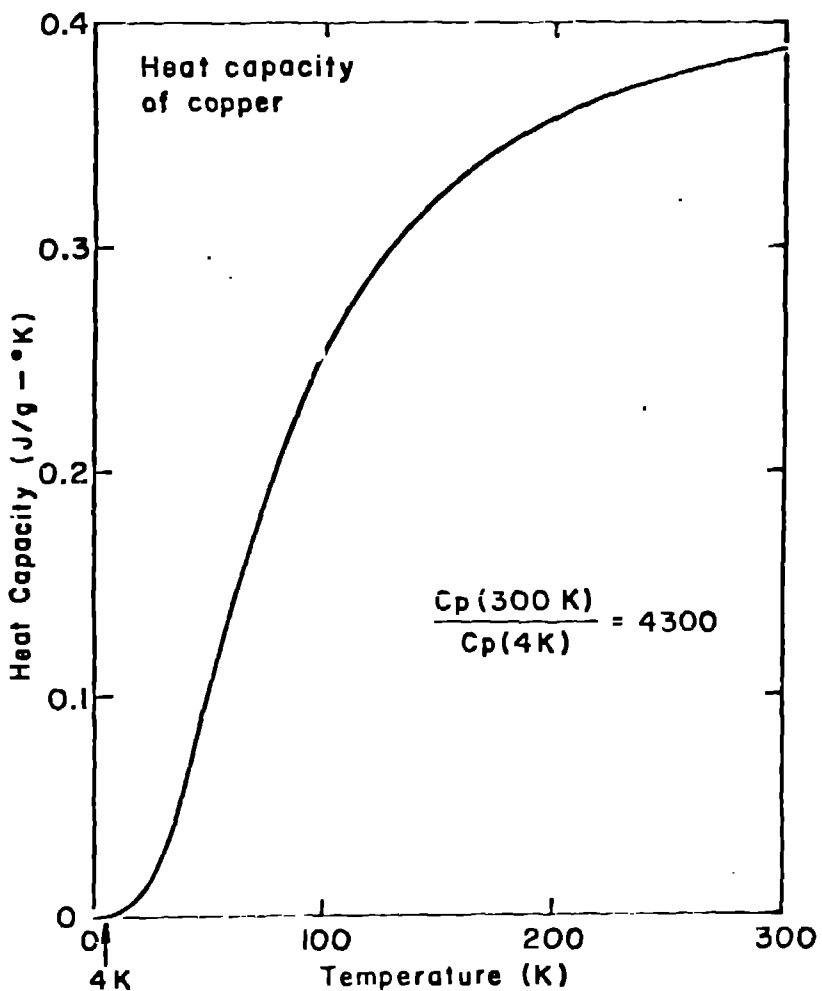


Fig. 1. Heat capacity of copper as a function of the absolute temperature. By operating the calorimeter at 4 K, the heat capacity of the 52 kg copper absorber was minimized. The temperature was stabilized by a liquid helium bath boiling at nearly constant pressure in a reservoir within the copper absorber. The absorbed decay heat evaporated liquid helium from the reservoir and a hot-film anemometer-type mass flowmeter measured the evolution of the boil-off gas. The flowmeter had a time constant of  $\sim 1$  ms. The pressure drop across the flowmeter at maximum flow ( $\sim 1$  liter/s) was  $\sim 1$  torr. This pressure change corresponds to a temperature change of  $\sim 1.7$  mK in the helium reservoir. Under these conditions, there is a minimum storage of thermal energy in the calorimeter, and a fast response time is possible. The high thermal conductivity of the very pure, well-annealed copper used for the absorber also contributed to the short time constant.

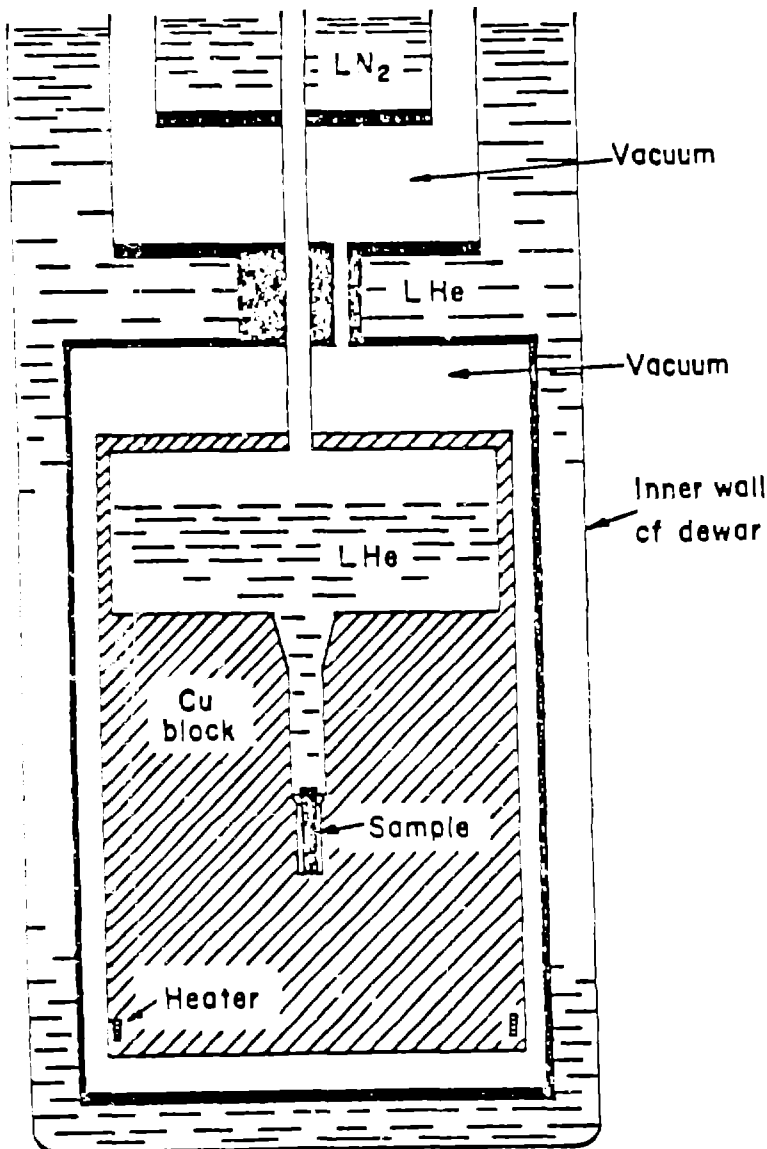


Fig. 2. Essential features of the calorimeter. The copper block, which absorbed > 97% of the radiation energy emitted by the sample, was 177.8 mm in diameter, 298.5 mm high, and weighed 52.008 kg. The reservoir in the top of the block was 3/4 filled with liquid helium. The block was suspended in vacuum by a 10-mm-i.d. thin-wall stainless steel tube which conducted the boil-off gas to a flowmeter at room temperature. The tube was also used to insert and remove samples and to transfer the liquid helium to the reservoir. A heater in the base of the block was used for calibration and testing. To prevent heat leak, a copper vacuum jacket, immersed in an outer liquid helium bath, surrounded the calorimeter block. A commercial liquid-nitrogen-jacketed dewar contained the entire assembly. All electrical leads reaching the calorimeter block passed through the outer helium bath, which intercepted heat conducted along them from warmer regions. The outer helium bath was kept 25mK above the temperature of the helium in the inner reservoir to prevent the boil-off gas from condensing on the tube walls after it left the reservoir. The boil-off gas was raised to room temperature in a controlled manner to minimize the effect of changes of temperature gradients along the gas-transport tube with boil-off gas flow rate.

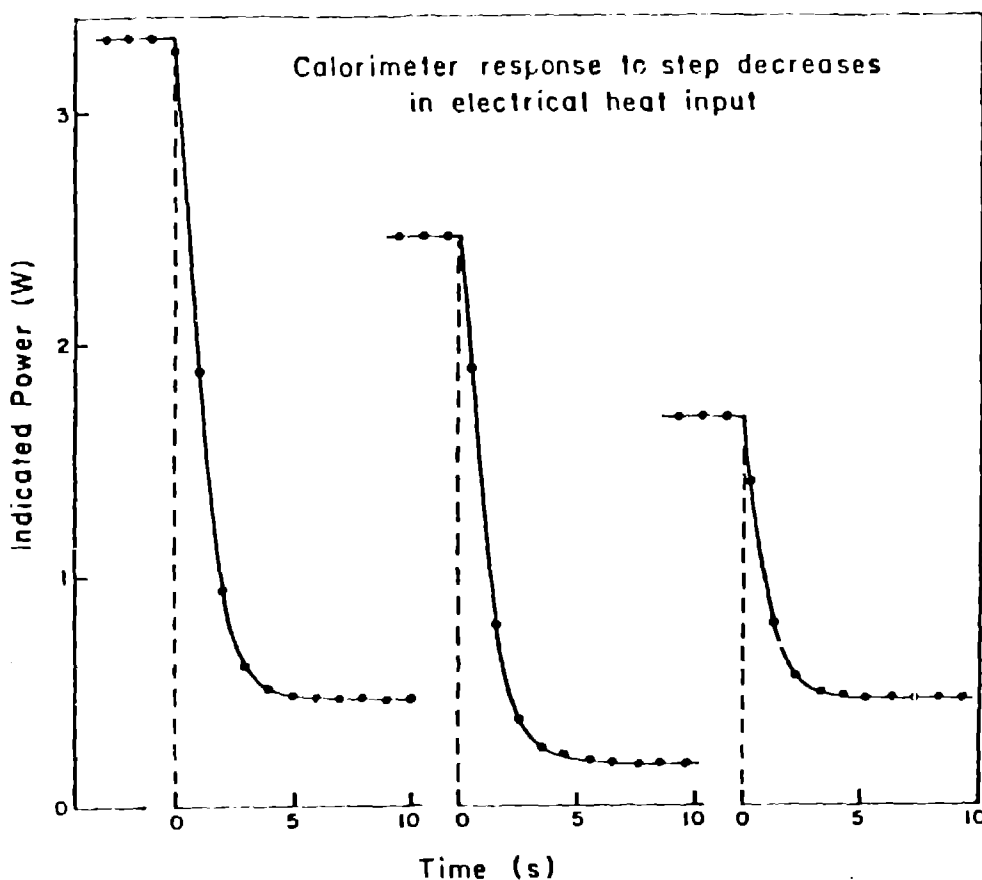
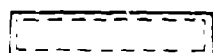
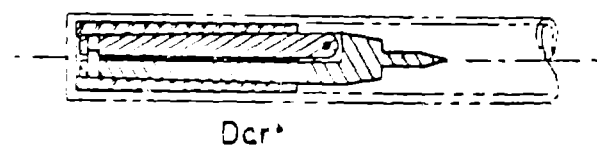


Fig. 3. Calorimeter response to step changes in electrical input. Step changes in electric heat input to the calorimeter were supplied via the electric heater embedded in the copper absorber block. For changes between power levels that were both  $> 70$  mW, the calorimeter response was well represented by a single exponential function. Ten measurements that included both increases and decreases in input power yielded a value of  $0.85 \pm 0.09$  s for the exponential response time. Below 70 mW, the anemometer flowmeter was no longer accurate. For powers below 70 mW, the boil-off flow rate was measured using an integrating volumetric flowmeter and a stopwatch. This caused no problems, since the decay heat was changing very slowly by the time ( $\sim 3 \times 10^4$  s) it had fallen to 70 mW. The electric heater was also used to determine an absolute calibration curve for the calorimeter. The calibration curve so obtained was in excellent agreement with one obtained from absolute gas-flow measurements using the well-known heat of vaporization of helium. The final calibration curve used in the determination of the  $^{235}\text{U}$  decay heat was a combination of the curves obtained by the two independent methods. In an additional measurement, the heat leak into the copper block was determined to be  $\leq 20$   $\mu\text{W}$  under the conditions of the experiment.



39 mm x 8 mm x 0.3 mm  
~ 60 mg 93%  $^{235}\text{U}$   
~ 240 mg Al clad

Sample



Dart

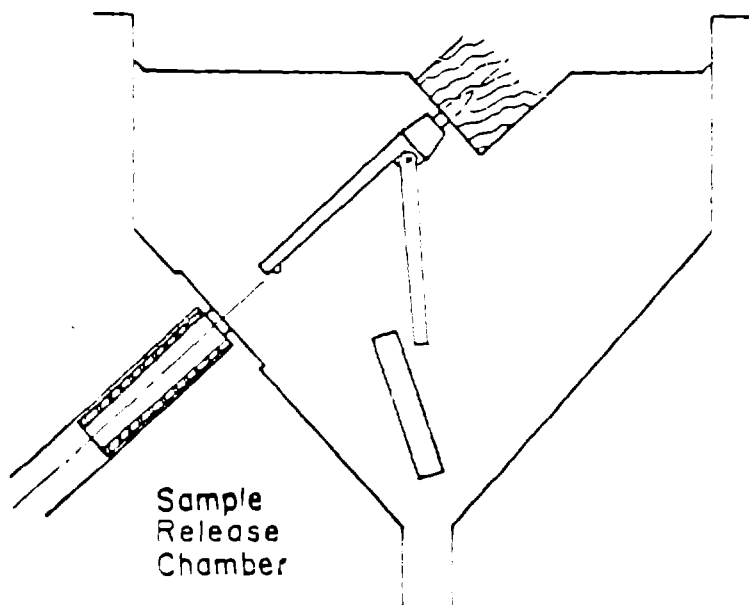


Fig. 4. Uranium - 235 sample and the system used to transport it from the irradiation position to the calorimeter. During irradiation, the sample was held between the hinged halves of an aluminum dart, which was clamped together by a tapered steel sleeve. After irradiation, the dart assembly was blown into the sample release chamber, where the sleeve was stripped off and the dart opened as it hit and stuck in a wooden target. Upon impact, the sample was released, then fell into the calorimeter through a ball valve that was opened at the correct time. The sample reached the liquid helium in the calorimeter ~ 1.5 s after the start of the ejection. It reached the temperature of the liquid helium ~ 3 s later. The ball valve remained open until the puff of gas from the sample cool-down had escaped; then it was closed, forcing the boil-off gas to pass through the flowmeter. During irradiation, helium gas flowed over the sample and through a charcoal trap near a NaI(Tl) radiation detector, which gave a prompt and sensitive indication of any escape of fission gases. Any samples that leaked were rejected. During the calorimetric measurements, the samples were at 4 K and all fission products were solids.

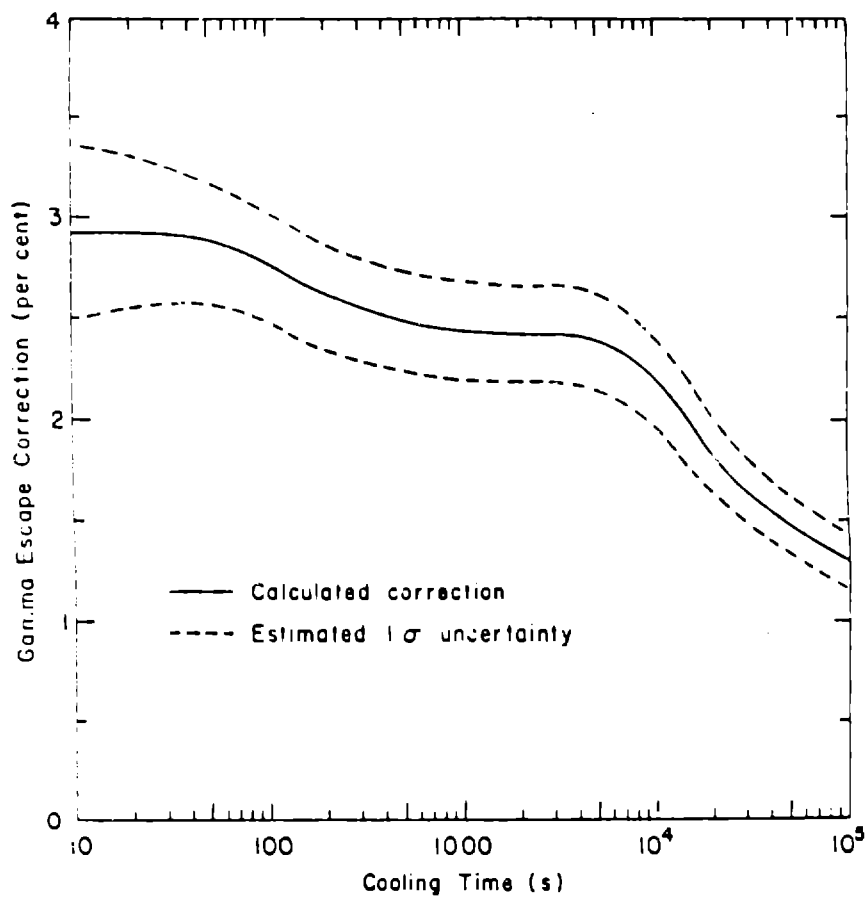
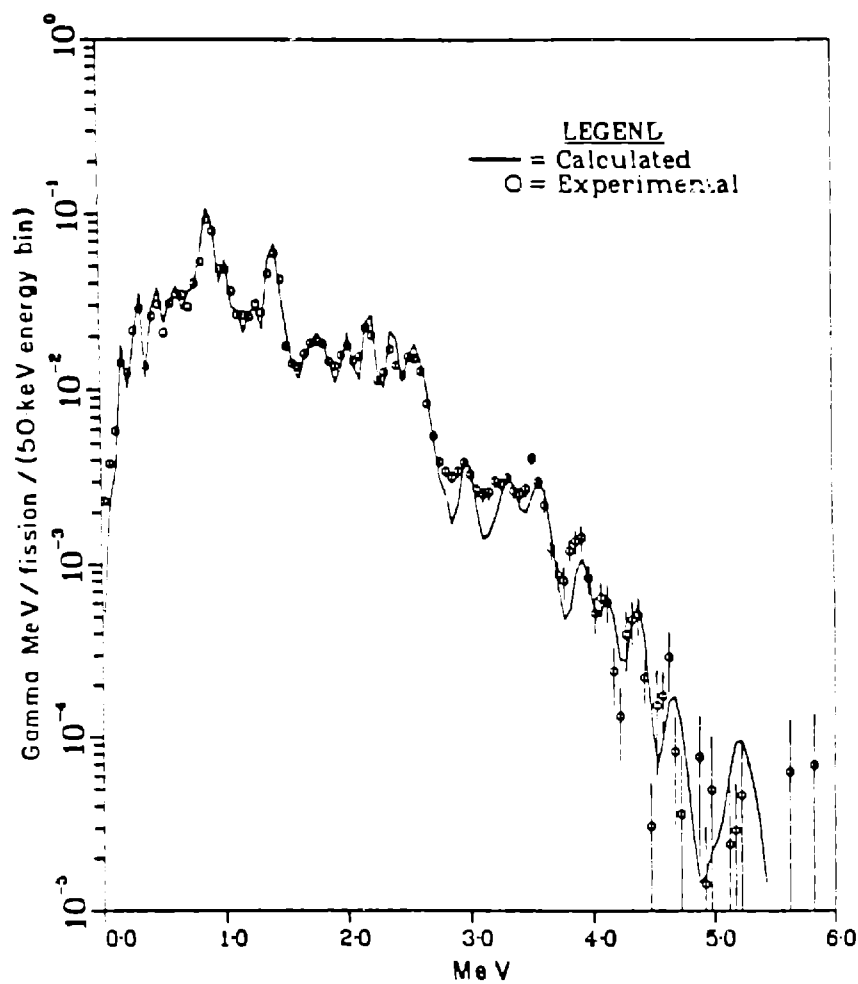


Fig. 5. Fission-product gamma spectrum (left) measured at a mean cooling time of 660 s after a  $2 \times 10^4$  s  $^{235}\text{U}$  irradiation. The solid curve was obtained from the ENDF/B-IV data base using a summation calculation. The correction for gamma escape from the calorimeter (right) was obtained from ten measured spectra using a Monte Carlo gamma transport calculation.

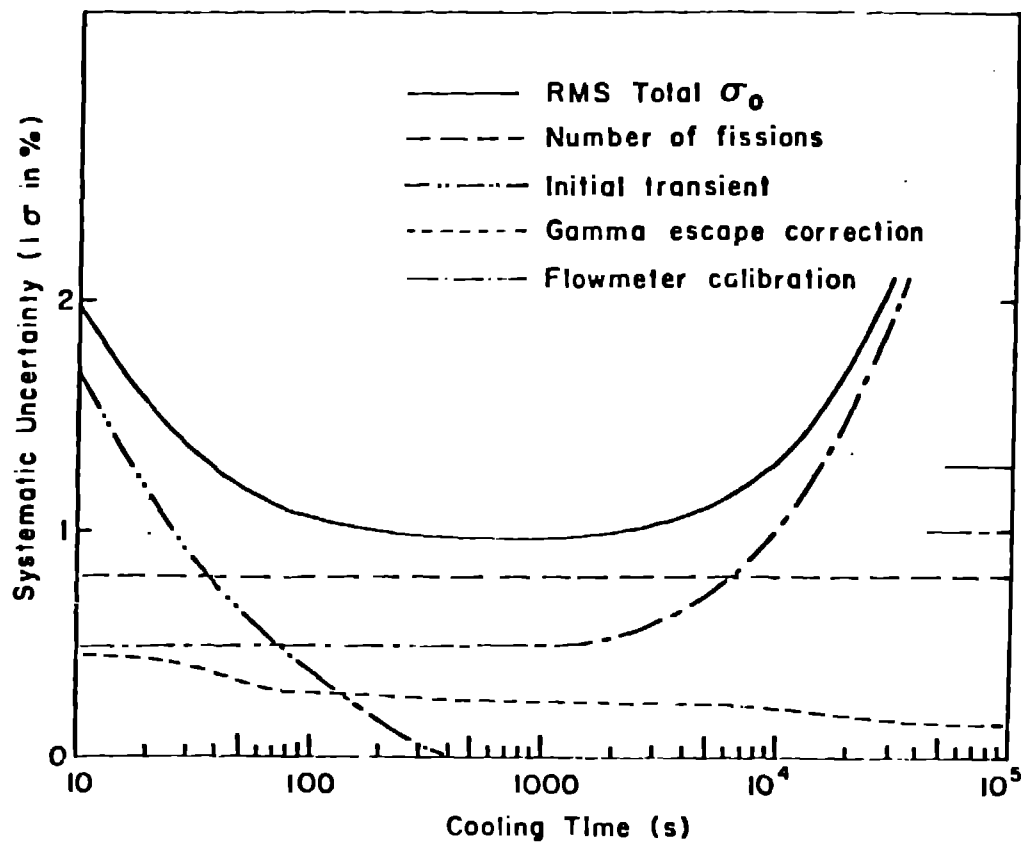


Fig. 6. Systematic uncertainties (those that do not contribute to the scatter in the data points at a given cooling time). The uncertainty in the number of fissions was estimated from an analysis of the calibration method used and from consistency checks with other Laboratories. The initial-transient correction consisted of (1) subtraction of the signal from an irradiated aluminum dummy sample and (2) an analytic correction based on the 0.85 s time constant of the calorimeter. The total initial-transient correction was assigned an uncertainty of 50% of its value. The gamma escape correction was assumed known to 15% of its value at the shortest cooling times, and to 10% of its value for cooling times  $> 70$  s. The flowmeter calibration curve uncertainty was estimated from the accuracy of the calibration standards and from the scatter of the calibration points around the fitted calibration curve. Flow measurements for  $t > 60\ 000$  s were made using an integrating volumetric flowmeter. Its uncertainty is shown by a separate part of the curve. Because they are uncorrelated, the total systematic uncertainty,  $\sigma_0$ , was taken to be the RMS sum of the individual systematic uncertainties.

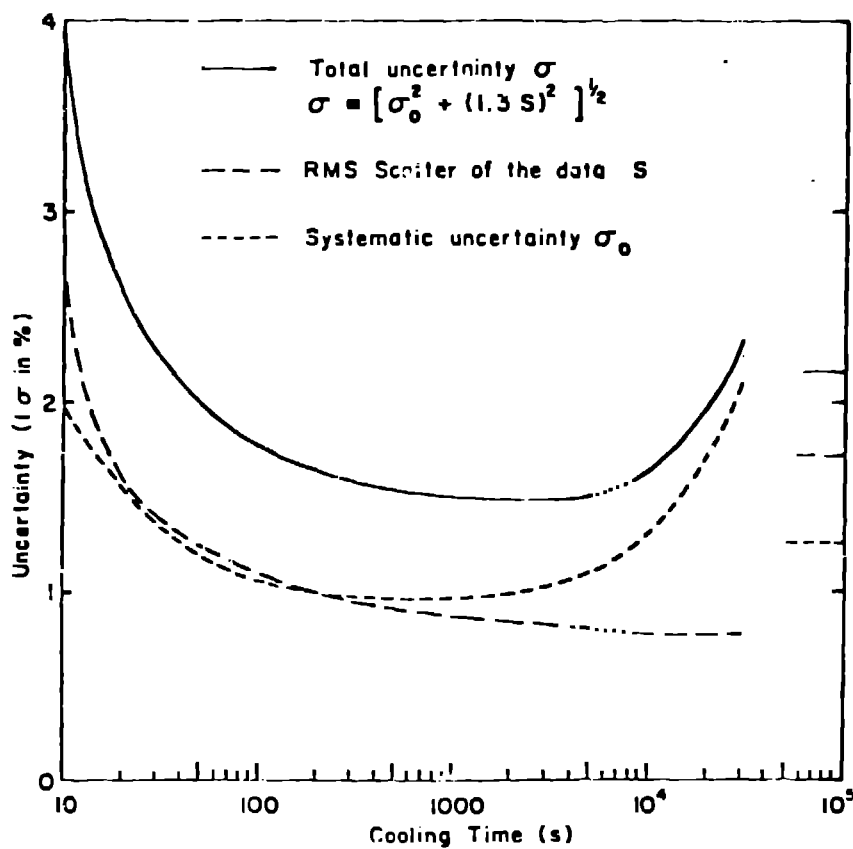


Fig. 7. Total uncertainty,  $\sigma$ , in the experimental data as estimated from the systematic uncertainty,  $\sigma_0$ , (Fig. 6.) and the RMS scatter,  $S$ , in the measurements made on different samples at the same cooling time. For most cooling times, data were obtained from three samples. When there were fewer than three data points,  $S$  was calculated by estimating the missing data points using nearby values from the same sample. Values of  $S$  larger than those shown on the curve were obtained for cooling times near 7000 s after the calorimeter was refilled with liquid helium. These times are indicated by dotted portions of the graph of  $S$ . The correct values were used in preparing Table I. To compensate for the small number of samples used (three), the experimental values of  $S$  were increased by a factor of 1.3 when the total uncertainty was calculated. All stated uncertainties are intended to represent one standard deviation of a normal distribution.

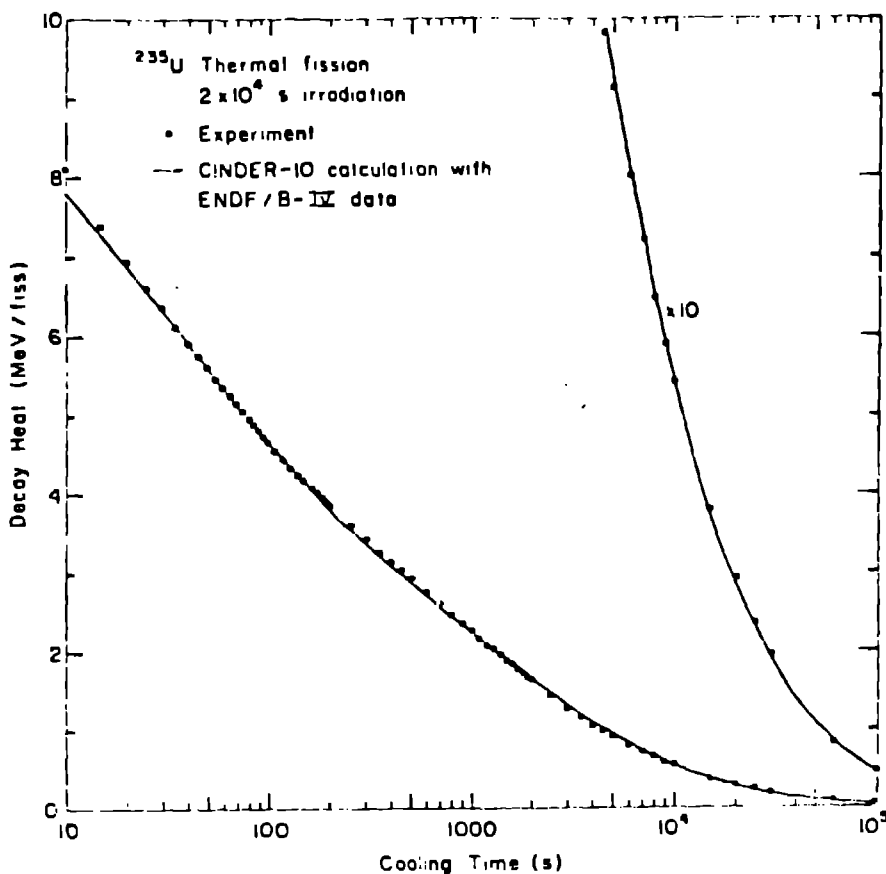


Fig. 8. Experimental and calculated decay heat for a  $2 \times 10^4$  s irradiation of  $^{235}\text{U}$  at constant thermal-neutron flux. The calculations used the ENDF/B-IV data base as listed and corrected by England and Schenter in Los Alamos Scientific Laboratory Report LA-6116-MS (ENDF-223). Measurements and calculations indicate that, under the conditions of the experiment, neutron capture in fission products, fission of  $^{238}\text{U}$ , and production of  $^{239}\text{U}$  and  $^{239}\text{Np}$  were all negligible. The calorimetric measurements were normalized to the fission rates in the samples determined by counting selected fission products subsequent to the calorimetric measurements. The isotopes  $^{99}\text{Mo}$  and  $^{140}\text{Ba}$  were beta-counted in chemically separated aliquots of the sample;  $^{95}\text{Zr}$ ,  $^{99}\text{No}$ ,  $^{140}\text{Ba-La}$ ,  $^{141}\text{Ce}$ , and  $^{147}\text{Nd}$  were gamma-counted in an unseparated aliquot. The fission determinations were calibrated against direct fission counting.

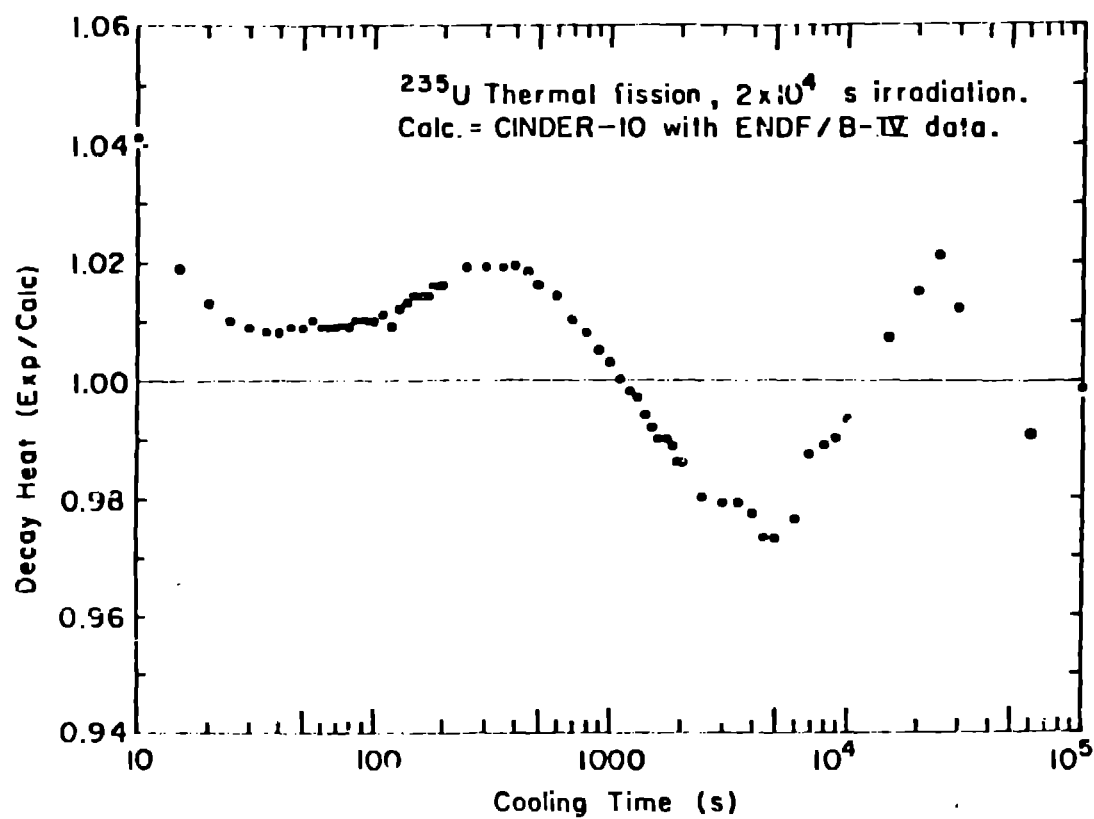


Fig. 9. Ratio of Experimental to calculated decay heat for a  $2 \times 10^4$  s  $^{235}\text{U}$  irradiation. To emphasize the small differences in the results shown in Fig. 8, the experimental data points have been divided by the summation calculation for the same cooling time and the ratios have been plotted on an expanded scale. The differences are well within the combined uncertainties for the experiment and the calculation.

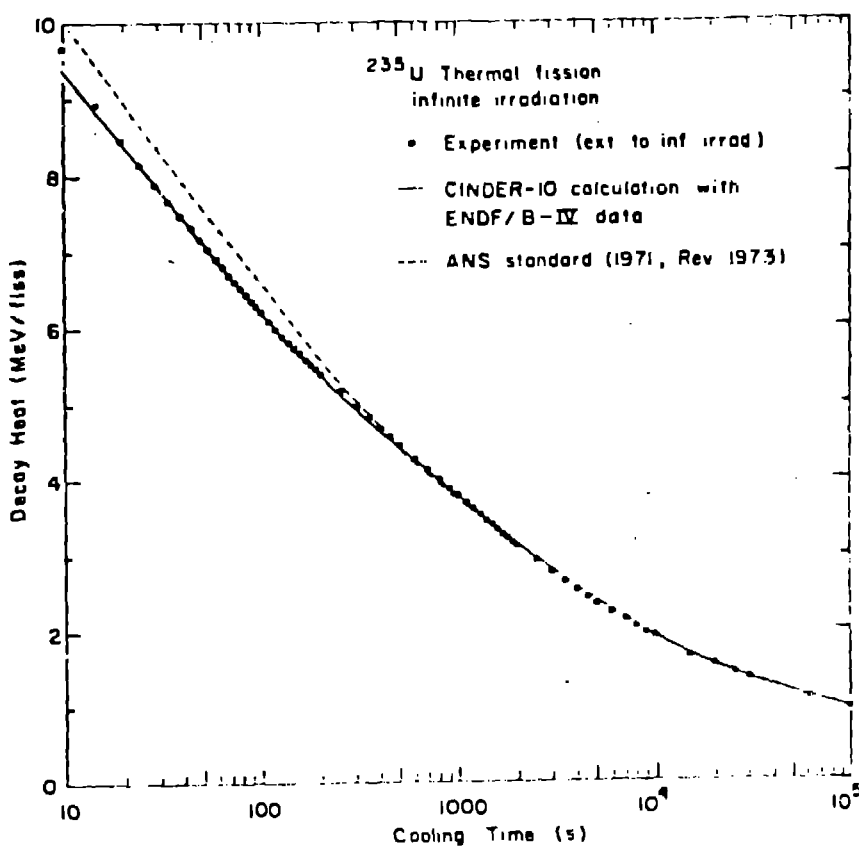


Fig. 10. Decay heat for infinite ( $10^{13}$  s) thermal-neutron irradiation of  $^{235}\text{U}$  at constant fission rate without neutron capture in fission products. The experimental data points have been extended to infinite irradiation by the addition of summation calculations made using the ENDF/B-IV data base. The calculational contribution to the infinite-irradiation decay heat was 16% at  $t = 10$  s, 51% at  $t = 2500$  s, and 95% at  $t = 10^5$  s. Also shown are the summation calculation and the present ANS Decay Heat Standard for infinite irradiation. It may be seen that the extended experimental data are in good agreement with the summation calculation, and are 7% below the standard at short cooling times. Moreover, the uncertainty associated with these measurements and calculations is significantly lower than that assigned to the standard. The ANS standard plus 20% is currently used for the decay heat source term in reactor safety evaluations.

TABLE  
EXPERIMENTAL AND CALCULATED DECAY HEAT FOR THE PRODUCTS OF THERMAL FISSION OF  $^{235}\text{U}$ .

Cooling Time (s)	2 x 10 <sup>4</sup> s Irradiation					Infinite Irradiation				
	Experimental Decay Heat (MeV/fiss)	Experimental Uncertainty (1 $\sigma$ in %)	Calculated Decay Heat		Ratio Exp/Calc Decay Heat	Experimental Decay Heat Extended by CINDER-10 and ENDF/B-IV (MeV/fiss)	Experimental Uncertainty <sup>a</sup> (1 $\sigma$ in %)	Calculated Decay Heat		Ratio Exp/Calc Decay Heat
			using CINDER-10	using ENDF/B-IV				using CINDER-10	using ENDF/B-IV	
10	8.30	4.1	7.780	1.041	9.65	3.5	9.327	1.035		
15	7.38	3.0	7.239	1.019	8.93	2.5	8.786	1.016		
20	6.933	2.6	6.842	1.013	8.480	2.2	8.389	1.011		
25	6.595	2.4	6.531	1.010	8.142	2.0				
30	6.335	2.3	6.276	1.009	7.882	1.9				
35	6.109	2.2	6.060	1.008	7.656	1.8				
40	5.920	2.1	5.873	1.008	7.467	1.7	7.420	1.006		
45	5.758	2.1	5.709	1.009	7.305	1.7				
50	5.614	2.0	5.562	1.009	7.160	1.6				
55	5.481	2.0	5.429	1.010	7.027	1.6				
60	5.358	2.0	5.309	1.009	6.904	1.6	6.855	1.007		
65	5.244	1.9	5.198	1.009	6.790	1.5				
70	5.141	1.9	5.097	1.009	6.687	1.5				
75	5.047	1.9	5.003	1.009	6.593	1.5				
80	4.958	1.8	4.915	1.009	6.504	1.5	6.461	1.007		
85	4.881	1.8	4.834	1.010	6.427	1.4				
90	4.806	1.8	4.758	1.010	6.351	1.4				
95	4.734	1.8	4.686	1.010	6.279	1.4				
100	4.667	1.8	4.619	1.010	6.212	1.4	6.164	1.008		
110	4.544	1.8	4.496	1.011	6.089	1.4				
120	4.426	1.7	4.385	1.009	5.971	1.4				
130	4.339	1.7	4.286	1.012	5.884	1.4				
140	4.251	1.7	4.195	1.013	5.795	1.4				
150	4.170	1.7	4.112	1.014	5.714	1.4	5.655	1.010		
160	4.092	1.7	4.035	1.014	5.636	1.4				
170	4.021	1.7	3.964	1.014	5.565	1.3				
180	3.960	1.7	3.899	1.016	5.503	1.3				
190	3.899	1.6	3.836	1.016	5.442	1.3				
200	3.841	1.6	3.780	1.016	5.384	1.3	5.323	1.011		
250	3.608	1.6	3.541	1.019	5.150	1.3				
300	3.419	1.6	3.355	1.019			5.323	1.011		
350	3.265	1.6	3.205	1.019	4.805	1.3				
400	3.135	1.6	3.078	1.019	4.673	1.3	4.616	1.012		
450	3.022	1.6	2.969	1.018	4.559	1.3				
500	2.920	1.6	2.873	1.016	4.456	1.3				
600	2.746	1.5	2.709	1.014	4.280	1.2	4.243	1.009		
700	2.598	1.5	2.572	1.010	4.130	1.2				
800	2.474	1.5	2.455	1.008	4.004	1.2	3.984	1.005		
900	2.363	1.5	2.351	1.005	3.890	1.2				
1000	2.264	1.5	2.258	1.003	3.789	1.2	3.783	1.002		

TABLE  
(continued)

Cooling Time (s)	2 x 10 <sup>4</sup> s Irradiation				Infinite Irradiation		
	Experimental Decay Heat (MeV/fiss)	Calculated Decay Heat		Ratio Exp/Calc	Experimental Decay Heat Extended by CINDER-10 and ENDF/B-IV (MeV/fiss)	Experimental Decay Heat from CINDER-10 and ENDF/B-IV (MeV/fiss)	Ratio Exp/Calc
		Experimental Uncertainty (1 $\sigma$ in %)	using CINDER-10 and ENDF/B-IV (MeV/fiss)				
1100	2.173	1.5	2.174	1.000	3.696	1.2	
1200	2.093	1.5	2.098	0.998	3.614	1.2	
1300	2.020	1.5	2.027	0.997	3.539	1.2	
1400	1.950	1.5	1.962	0.994	3.467	1.2	
1500	1.886	1.5	1.901	0.992	3.401	1.2	3.416 0.996
1600	1.827	1.5	1.845	0.990	3.340	1.2	
1700	1.773	1.5	1.791	0.990	3.284	1.2	
1800	1.721	1.5	1.741	0.989	3.229	1.2	
1900	1.671	1.5	1.694	0.986	3.177	1.2	
2000	1.627	1.5	1.650	0.986	3.131	1.2	3.154 0.993
2500	1.431	1.5	1.460	0.980	2.925	1.3	
3000	1.283	1.5	1.311	0.979	2.768	1.3	
3500	1.166	1.5	1.191	0.979	2.641	1.3	
4000	1.067	1.5	1.092	0.977	2.533	1.3	2.557 0.991
4500	0.9808	1.5	1.008	0.973	2.438	1.3	
5000	0.9111	1.5	0.9362	0.973	2.360	1.3	
6000	0.7998	2.3	0.8198	0.976	2.231	1.5	2.251 0.991
7000	0.7195	2.0	0.7287	0.987	2.135	1.5	
8000	0.6480	1.6	0.6553	0.989	2.049	1.5	2.056 0.997
9000	0.5886	1.6	0.5948	0.990	1.975	1.5	
10000	0.5401	1.7	0.5440	0.993	1.912	1.5	1.916 0.998
15000	0.3803	1.8	0.3778	1.007	1.691	1.6	1.689 1.001
20000	0.2918	2.0	0.2874	1.015	1.552	1.7	1.547 1.003
25000	0.2359	2.2	0.2311	1.021	1.453	1.7	
30000	0.1947	2.3	0.1923	1.012	1.375	1.7	
62183	0.0822	2.2	0.0832	0.988	1.105	1.9	
100000	0.0454	2.2	0.0455	0.998	0.971	1.9	0.969 1.002

\*Calculated on the assumptions that the calculated infinite irradiation decay heat curve has 2% uncertainty for  $t_{cool} \geq 2 \times 10^4$  s, and that this uncertainty is uncorrelated with the experimental uncertainty.